Novel Mathematical Model for Predicting the Dissolution Profile of Spherical Particles under Non-sink Conditions

Yasuyoshi Agata, Yasunori Iwao,* Atsuo Miyagishima, and Shigeru Itai

School of Pharmaceutical Sciences, University of Shizuoka; 52–1 Yada, Suruga-ku, Shizuoka 422–8526, Japan.
Received November 16, 2009; accepted December 28, 2009; published online January 8, 2010

A mechanistic mathematical model was designed to predict dissolution patterns under non-sink conditions. Sulfamethoxazole was used as a model drug, and its physico-chemical properties such as solubility, density, and intrinsic dissolution rate constant *etc.*, were investigated in order to apply these experimental values to the proposed model. Dissolution tests were employed as a way of validating the mathematical model, and it was found that the predictions given by the model were surprisingly accurate for all particle sizes. In addition, a simulation focused on forecasting the fraction of the drug that was dissolved at a certain time point when various initial particle diameters were used was also particularly valuable. Therefore, these results demonstrated that the model enables dissolution profiles to be analyzed under non-sink conditions.

Key words mathematical model; non-sink condition; sulfamethoxazole; dissolution rate control

The quantitative prediction of drug dissolution profiles is critically important for elucidating the pharmacokinetic behavior of drugs. The determination of drug dissolution *in vitro* is one of the key elements in the pharmaceutical development process and is sometimes used as a surrogate for the assessment of bioequivalence. Therefore, many mathematical models for predicting drug dissolution, which can be roughly categorized into mechanistic and empirical methods, have been proposed.

The basic mechanistic models for solid dissolution were developed by Noyes–Whitney[1] and later Nernst[2] and Brunner.[3] These familiar models are known as "diffusion-controlled models" today. Furthermore, based on these models, the "cube-root law" devised by Hixson and Crowell[4] and other equations[5,6] were developed. One of the significant advantages of these mechanistic models is that they allow easy prediction of a drug dissolution profile without requiring a dissolution test because physical parameters such as solubility, density, diffusivity *etc.*, which are components of the equations, can be determined by more convenient experiments. In addition, since the crucial parameters that influence drug dissolution patterns have been clarified, the models may be useful for controlling drug dissolution patterns. Although, to the best of our knowledge, perfect sink conditions, in which the bulk concentration of a drug is considerably less than its solubility, have been universally assumed in these models, discrepancies between the theoretical and experimental data have been found for water-insoluble drugs, suggesting that the development of new mechanistic models for predicting almost all kinds of drug dissolution is desired.

On the other hand, empirical and semiempirical models, not mechanistic models, have also been developed by numerous researchers.[7,10,11] A general empirical equation called the Weibull model has been applied to the drug dissolution process by Langenbucher,[7] and this model can be adapted to almost all kinds of drug dissolution (Goldsmith *et al.*,[8] Vudathala and Rogers[9]). Korsmeyer *et al.*[10,11] also developed a semiempirical model called the Korsmeyer–Peppas model. This Korsmeyer–Peppas model is surprisingly simple, but is capable of predicting many kinds of drug dissolution profiles. Although both the Weibull and Korsmeyer–Peppas models are able to describe drug dissolution profiles even if the drug is water-soluble or not, a dissolution test is required to determine the parameters of the equations because these models are not mechanistic. Therefore, empirical and semiempirical models are difficult to apply to the control of drug dissolution patterns as desired.

It has been estimated that more than 40% of the new chemical entities developed through a high throughput drug discovery program have poor water solubility.[12,13] In order to effectively develop pharmaceutical products, the establishment of a new mechanistic model that is independent of drug solubility is desired. The purpose of the present study is to derive an adequate equation that describes the dissolution patterns of poorly water-soluble drugs under non-sink conditions and to validate the equation experimentally using sulfamethoxazole (SMX) as a model drug.

Theory The amount (W) of a drug flowing through a unit cross-section of the available surface area (S) in unit time (t) is known as flux (J).

$$J = \frac{dW}{Sdt} \tag{1}$$

Based on Fick's first law, flux is expressed as follows:

$$J = -D\frac{dC}{dx} \tag{2}$$

in which D is the diffusion coefficient of a drug molecule, C is its concentration, and x is the distance moved perpendicular to the available surface.

Using the following assumptions, Eq. 2 becomes Eq. 3.

- The particle is in a well-stirred solution, and a boundary layer of constant thickness (h) exists around the particle.
- The concentration at the interface between the solid and the solution is saturated (C_s), and solubility is independent of particle size.
- During dissolution, a pseudo-steady-state is established with only minimal solid dissolution, after which the overall mass transport rates across the inner and outer surfaces of the diffusion layer are assumed to be equal.

* To whom correspondence should be addressed. e-mail: yasuiwao@u-shizuoka-ken.ac.jp

$$J = \frac{D}{h}(C_s - C) \tag{3}$$

where C is bulk solution concentration. Substituting Eq. 1 into Eq. 3 gives:

$$\frac{dW}{dt} = -kS(C_s - C) \tag{4}$$

where k represents the dissolution rate constant per unit area (intrinsic dissolution rate constant) ($k=D/h$). Since sink conditions, in which the bulk concentration of a drug (C) is considerably less than its solubility (C_s), have been universally assumed (Fig. 1a), term (C_s-C) of Eq. 4 is approximated by C_s. However, in the present study, this term is not approximated since we assumed the non-sink conditions, in which there are not significant differences between C and C_s, as illustrated in Fig. 1b.

On the other hand, for N monodispersed spherical particles, the drug amount present in the system is:

$$W = \frac{N\pi\rho}{6} X^3 \tag{5}$$

where ρ is the density of the particle, and X is the diameter of particle.

Differentiating both sides of Eq. 5 with time gives:

$$\frac{dW}{dt} = \frac{N\pi\rho}{2} X^2 \frac{dX}{dt} \tag{6}$$

Here, we assume that the available surface area (S) is equal to the particle surface area:

$$S = N\pi X^2 \tag{7}$$

From Eqs. 4, 6, and 7, we get the following ordinal differential equation:

$$\frac{dX}{dt} = -\frac{2k}{\rho}(C_s - C) \tag{8}$$

Using X_0 for the initial particle diameter and V for the volume of solvent, concentration C is represented as:

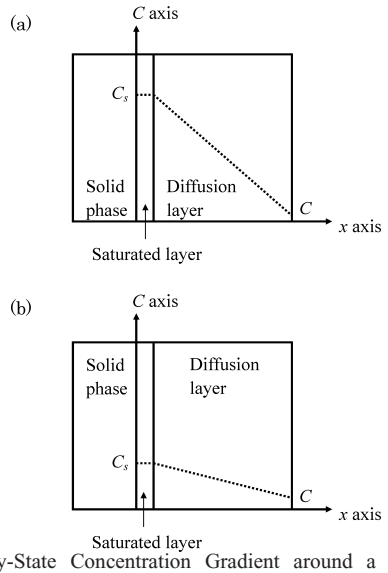

Fig. 1. Steady-State Concentration Gradient around a Planar Surface under Sink Conditions (a) and Non-sink Conditions (b)

$$C = \frac{N\pi\rho}{6V}(X_0^3 - X^3) \tag{9}$$

Substituting Eq. 9 into Eq. 8 gives:

$$\frac{1}{a + bX^3}\frac{dX}{dt} = -\frac{2k}{\rho} \tag{10}$$

where a and b are constants:

$$a = C_s - \frac{N\pi\rho}{6V} X_0^3 \tag{11}$$

$$b = -\frac{N\pi\rho}{6} \tag{12}$$

Solving Eq. 10 gives:

$$F(X) - F(X_0) = -\frac{2k}{\rho} t \tag{13}$$

where the function F is defined as follows:

$$F(X) = \frac{1}{6b}\left(\frac{b}{a}\right)^{2/3}\left[\ln\frac{\{X - (a/b)^{1/3}\}^2}{X^2 - (a/b)^{1/3}X + (a/b)^{2/3}} + 2\sqrt{3}\arctan\left(\frac{2}{\sqrt{3}}(b/a)^{1/3}X - \frac{1}{\sqrt{3}}\right)\right] \tag{14}$$

The symbolic calculus was conducted using Maple. Rearranging Eq. 13 gives:

$$X = F^{-1}\left(F(X_0) - \frac{2k}{\rho} t\right) \tag{15}$$

where F^{-1} is the inverse function of the function F.

The fraction of the drug dissolved (%*Dissolved*) is defined using Eq. 15:

$$\%Dissolved = 100\left[1 - \frac{1}{X_0^3}\left\{F^{-1}\left(F(X_0) - \frac{2k}{\rho} t\right)\right\}^3\right] \tag{16}$$

where $F^{-1}(X)$ was calculated using the software Excel and Maple.

The fraction of the drug dissolved under sink conditions (%$Dissolved_{\text{sink}}$) can also be derived from the cube-root law:

$$\%Dissolved_{\text{sink}} = 100\left(1 - \frac{2kC_s}{\rho X_0} t\right)^3 \tag{17}$$

Experimental

Materials Sulfamethoxazole (SMX) was purchased from Wako Pure Chemical Ind. Ltd. (Osaka, Japan). All of the reagents used were of the highest grade available from commercial sources.

Preparation of SMX SMX crystals were prepared by the recrystallization method. Briefly, after SMX had been completely dissolved in boiled ethanol, the solution was filtered immediately. The filtrate was then spontaneously cooled to room temperature. The separated SMX crystals were then recovered and desiccated for 3 h at 40 °C. After drying-out the SMX crystals, they were classified by sieving. Next, the sieved crystals were washed with distilled water to remove the micro particles adhered to their surfaces and then desiccated for 3 h at 40 °C.

Dissolution Study The dissolution behavior of SMX was examined in accordance with the paddle method listed in the Japanese Pharmacopoeia (15th edition). The test solution was 900 ml phosphate buffer saline (PBS; pH 7.4) containing 15 v/v % ethanol at 30.0±0.5 °C, and the paddle rotation speed was 50 rpm. At 1, 3, 5, 10, 15, and 20 min, the samples (5 ml) were

withdrawn. The solution was then filtered through a membrane filter (0.45 μm). Then, the absorbance was determined at 264 nm with a spectrophotometer (UVmini, SHIMADZU), and the SMX concentration was calculated from the absorbance of a standard solution.

Determination of Initial Particle Diameter About 40 mg of SMX were measured, and the number of particles was counted with the eye. The initial particle diameter, X_0, was obtained using the following equation:

$$X_0 = \sqrt[3]{\frac{6w}{n\pi\rho}} \tag{18}$$

where w is the mass of SMX, n is the number of the particles, and ρ is the density of SMX.

Determination of the Solubility of SMX Three-hundred milligrams of SMX were added to 50 ml of pH 7.4 PBS containing 15 v/v% ethanol at 30 °C, and the mixture was agitated for 48 h. The solubility of SMX was determined in the same manner as described in the dissolution study.

Determination of the Dissolution Rate Constant per Unit Area In order to determine k, the fixed disk method was used. An SMX disk with a diameter of 1.3 cm (surface area=1.33 cm^2) was prepared by compressing 400 mg of the drug powder at a pressure of 1 tf. The disk was placed in a JP dissolution test apparatus and rotated at 50 rpm in PBS at pH 7.4 and 30 °C. Five milliliters of the solution were withdrawn at appropriate intervals and, after adequate dilution, the SMX concentration was calculated spectrophotometrically by the same method as used in the dissolution study.

Determination of Density SMX density was measured using a pycnometer.

Results and Discussion

Determination of Physico-chemical Parameters of SMX Figure 2 shows the dissolution profile of SMX in a fixed disk with a surface area of 1.33 cm^2. From the Nernst equation, the following Eq. 19 was obtained[14] and then was fitted to the experimental data using the least squares method.

$$\ln \frac{C_s}{C_s - C} = \frac{kS}{V} t \tag{19}$$

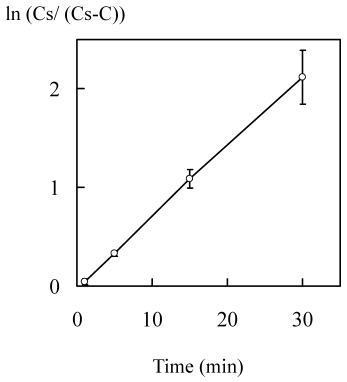

Fig. 2. Dissolution Profile of SMX from a Fixed Disk with an Available Surface Area of 1.33 cm^2

Open circles: experimental values, solid line: Eq. 19. Each symbol represents the mean±S.D. (n=3).

Table 1. Physico-chemical Parameters of SMX

Solubility (C_s)	5.30 μg/l
Density of particles (ρ)	1.32 g/cm^3
Rate constant (k)	0.048 cm/min

Table 2. Initial Diameter of Sieved SMX

Fraction	Number of particles (number/g)	Initial diameter (μm)
300—420 μm	24963	387
500—600 μm	10290	520
600—710 μm	6437	608

As shown in Fig. 2, good agreement was observed between the theoretical (solid line) and experimental values (symbols). From the slope of Eq. 19, k was determined. The value of k as well as the solubility and the density of the particles are shown in Table 1. Table 2 also shows the initial diameters of the sieved particles as calculated by Eq. 18.

Application of the Mathematical Model to the Dissolution Behavior of SMX Particles Figure 3a shows the dissolution behavior of SMX particles with an initial diameter of 387 μm. The broken and solid curves represent the theoretical values predicted under sink conditions by Eq. 17 and under non-sink conditions by Eq. 16, respectively, and the symbols represent the experimentally obtained data. Good agreement was observed between the theoretical values under non-sink conditions (solid curve) and the experimental values (symbols); whereas, a significant deviation from the theoretical values was observed under sink conditions (broken curve). As the cube-root law (Eq. 17) was originally applied to compounds with relatively high water solubility, it might be inappropriate to apply it to high doses of poorly water-soluble drugs. In addition, Figs. 3b and c show the dissolution behaviors of SMX with initial particle diameters of 520 μm and 608 μm, respectively. As expected, good agreement was obtained between the theoretical values under non-sink conditions (solid curve) and the experimental values (symbols) in both cases, suggesting that the equation derived in the present study is able to predict the dissolution profile of SMX. Furthermore, since this mathematical model was derived without assuming specific physico-chemical properties of SMX, it is considered that this model could allow the prediction of the dissolution profile of other water-insoluble drugs.

However, the experimental values of SMX dissolution at the early and late stages were shown to be slightly higher and lower, respectively, than the predicted values. These deviations may have been caused by the particle size inhomogeneity. Namely, in this study, since we classified the SMX particles by sieving, SMX particle size inhomogeneity remained to some degree. To easily understand this phenomenon, a schematic explanation of the changes in particle size that occurred throughout the dissolution study was constructed (Fig. 4). First, we defined a numerical size distribution function (n) as follows:

$$n(X) = \begin{Bmatrix} N_L\,(X = X_L) \\ N_S\,(X = X_S) \\ 0\ \text{(otherwise)} \end{Bmatrix} \tag{20}$$

where N_L is the number of particles with a larger initial diameter of X_L, and N_S is the number of particles with smaller initial diameter of X_S. The sum of N_L and N_S must equal N (Eq. 21a).

$$N_L + N_S = N \tag{21a}$$

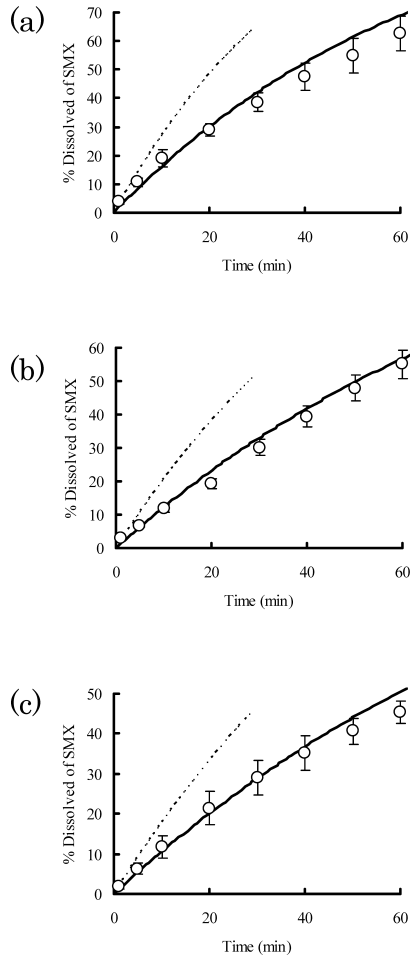

Fig. 3. Dissolution Profile of SMX Particles with Initial Particle Diameters of 387 μm (a), 520 μm (b), and 608 μm (c)

Open circles: experimental values, solid curve: prediction under non-sink model, broken curve: prediction under sink model. Each symbol represents the mean±S.D. (n=3).

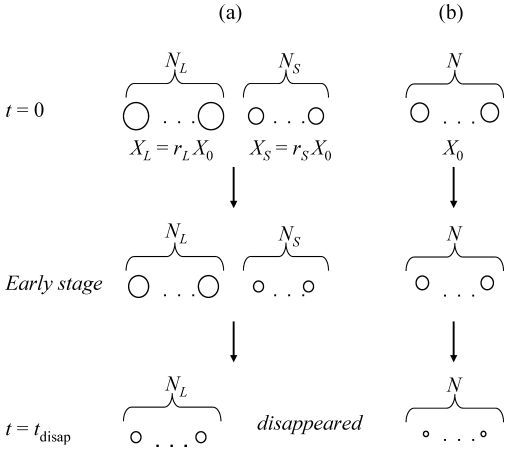

Fig. 4. Schematic Explanation of Changes in Particle Size throughout the Dissolution Study

(a) In the presence of a range of particle sizes and (b) when using a uniform particle size.

N_L and N_S are also constrained by the following equation:

$$\frac{N_L}{N_L+N_S}r_L^3+\frac{N_S}{N_L+N_S}r_S^3=1 \tag{21b}$$

in which r_L and r_S are the coefficients that satisfy the following equations:

$$r_L=\frac{X_L}{X_0} \tag{22}$$

$$r_S=\frac{X_S}{X_0} \tag{23}$$

If a theoretical system satisfies Eqs. 20—23, the mass of the particles in the system (w) is given by:

$$w=\frac{N_L\pi\rho}{6}X_L^3+\frac{N_S\pi\rho}{6}X_S^3=\frac{N\pi\rho}{6}X_0^3 \tag{24}$$

Figure 4a shows a schematic explanation of this system, and Fig. 4b shows the conditions assumed by Eq. 16. The model derived in this study cannot distinguish between Figs. 4a and b, which gave us identical predictions. However, at the early stage of dissolution, the experimental values of SMX dissolution were slightly higher. Since the rate of dissolution is affected by S as shown in Eq. 4, the sum of the available surface area of X_S and X_L might be larger than that of X_0, and consequently higher dissolution might be observed. However, this tendency will be changed with time, especially when $t=t_{\mathrm{disap}}$, where t_{disap} is the time when a smaller proportion of the drug has disappeared. The disappearance of a smaller fraction of the drug considerably decreases the available surface area. Therefore, the dissolution rate decreases too, and lower dissolution is observed. Therefore, it was found that since particles with a range of sizes were applied to this system, an unsatisfactory result might be obtained during the early and late stages of dissolution.

Effect of Initial Particle Size on the Dissolution Behavior of SMX In Eq. 16, the parameters C_s, ρ, and k are characterized by a combination of the drug used and the conditions of the system (solvent, paddle speed), and N is restricted by the initial dose and initial diameter (Eq. 18). However, since the initial diameter X_0 is only an arbitrary parameter, setting the initial diameter is a way of controlling drug dissolution patterns. Treating t as a constant (τ) and X_0 as a variable, Eq. 16 can be regarded as a function of X_0, as shown in Eqs. 25 and 26.

$$X=F^{-1}\left(F(X_0)-\frac{2k}{\rho}\tau\right) \tag{25}$$

$$\%Dissolved=100\left[1-\frac{1}{X_0^3}\left\{F^{-1}\left(F(X_0)-\frac{2k}{\rho}\tau\right)\right\}^3\right] \tag{26}$$

Using this manner, we could resolve some drug development problems. For example, imagine a situation in which more than 85% of a generic drug needs to be dissolved within 15 min in order to achieve bioequivalence. The question is what size of particle is needed to achieve this goal. Figure 5 shows the *%Dissolved* of SMX at τ=15 in the case of an initial dose of 2.5 g. As shown in Fig. 5, the initial diameter that provides the desired dissolution behavior is less than 66 μm.

Conclusions

We have developed a novel equation that describes the dissolution profiles of water-insoluble drugs, and the equation has been validated experimentally. Furthermore, deeper insight into the dissolution of particles was obtained from the

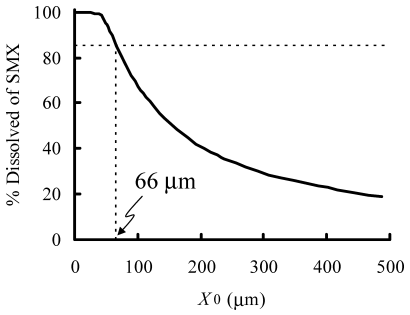

Fig. 5. Simulated %*Dissolved* of SMX after 15 min of a Dissolution Test
The initial amount of SMX was 2.5 g.

equation. Therefore, the equation enables the analysis of dissolution profiles under non-sink conditions.

References

1) Noyes A., Whitney W. R., *J. Am. Chem. Soc.*, **19**, 930—934 (1897).
2) Nernst W., *Z. Phys. Chem.*, **47**, 52—55 (1904).
3) Brunner E., *Z. Phys. Chem.*, **47**, 56—102 (1904).
4) Hixson A. W., Crowell J. H., *Ind. Eng. Chem.*, **23**, 923—931 (1931).
5) Niebergall P. J., Milosovich G., Goyan J. E., *J. Pharm. Sci.*, **52**, 236—241 (1963).
6) Higuchi W. I., Hiestand E. N., *J. Pharm. Sci.*, **52**, 67—71 (1963).
7) Langenbucher F., *J. Pharm. Pharmacol.*, **24**, 979—981 (1972).
8) Goldsmith J. A., Randall N., Ross S. D., *J. Pharm. Parmacol.*, **30**, 289—297 (1978).
9) Vudathala G. K., Rogers J. A., *J. Pharm. Sci.*, **82**, 282—286 (1992).
10) Korsmeyer R. W., Gurny R., Doelker E., Buri P., Peppas N. A., *Int. J. Pharm.*, **15**, 25—35 (1983).
11) Peppas N. A., *Pharm. Acta Helv.*, **60**, 110—111 (1985).
12) Lipinski C. A., *Curr. Drug Discov.*, **2001**, 17—19 (2001).
13) Lipinski C. A., *Am. Pharm. Rev.*, **5**, 82—85 (2001).
14) Yajima T., Nagata A., Demachi M., Umeki N., Iai S., Yunoki N., Nemoto M., *Chem. Pharm. Bull.*, **44**, 187—191 (1996).